ChemComm

COMMUNICATION

View Article Online
View Journal | View Issue

Cite this: *Chem. Commun.*, 2016, 52, 12438

Received 15th August 2016,
Accepted 27th September 2016

DOI: 10.1039/c6cc06706a

www.rsc.org/chemcomm

Anion size control of the packing in the metallic *versus* semiconducting chiral radical cation salts $(DM\text{-}EDT\text{-}TTF)_2XF_6$ (X = P, As, Sb)†

Flavia Pop,[a] Pascale Auban-Senzier,[b] Enric Canadell[c] and Narcis Avarvari*[a]

Control of the structural type in metallic enantiopure and racemic radical cation salts is achieved through hydrogen bonding interactions between the chiral donor DM-EDT-TTF and the XF_6 anions (X = P, As, Sb), determined by the anion size and the chiral information.

Chiral tetrathiafulvalenes (TTF) have attracted much attention especially in the last decade,[1] as they can provide chiral crystalline molecular conductors which, among other interesting features, should in principle show electrical magneto-chiral anisotropy (eMChA), recently observed for the first time in TTF based materials.[2] The corresponding enantiomeric conductors $(DM\text{-}EDT\text{-}TTF)_2ClO_4$ have been obtained by electrocrystallization of either (*S*,*S*) and (*R*,*R*) dimethyl-ethylenedithio-tetrathiafulvalene (DM-EDT-TTF) (Scheme 1). Here the chirality conferred by the two stereogenic carbon atoms has been transferred at the microscopic scale providing enantiomorphic crystals.

While chirality in TTF precursors has been introduced through various functions such as stereogenic carbon atoms,[1,3–6] sulfoxides,[7] allenes,[8] binaphthyls,[9] helicenes,[10] *para*-cyclophanes,[11] and even expressed at supramolecular level in helical aggregates,[12] examples of conducting chiral radical cation salts are still rare comparatively. Beside the ones derived from DM-EDT-TTF,[2] they include those prepared out of dimethylated (DM-BEDT-TTF)[13] and tetramethylated bis(ethylenedithio)-tetrathiafulvalene (TM-BEDT-TTF),[14] the last donor representing the first reported enantiopure TTF derivative.[15] Besides the manifestation of eMChA, which is a synergistic effect of the chirality on the resistivity of chiral conductors measured in a magnetic field collinear with the current,[16] the conductivity

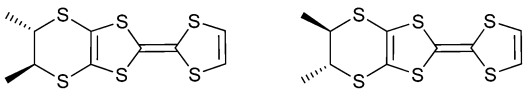

(*S*,*S*)-DM-EDT-TTF
(*S*,*S*)-**1**

(*R*,*R*)-DM-EDT-TTF
(*R*,*R*)-**1**

Scheme 1 Enantiopure dimethyl-ethylenedithio-tetrathiafulvalene (DM-EDT-TTF).

of enantiopure conductors can be higher than that of the racemic counterparts when structural disorder is present in the latter despite identical cell parameters and donor anion ratio. Such differences have been observed in enantiomeric and racemic radical cation salts based either on TTF-oxazolines[17] or TM-BEDT-TTF.[18] However, in the absence of crystalline disorder the conducting properties of the enantiopure and racemic forms were found to be similar.[14b,19] Less often is the case where enantiopure and racemic salts prepared from the same donor in the same conditions show completely different packings. In this respect we have recently described the complete series of radical cation salts $(DM\text{-}EDT\text{-}TTF)_2PF_6$ for which the enantiopure compounds crystallized in the monoclinic space group $P2_1$ with four independent donor molecules and two anions in the unit cell, while the racemic salt crystallized in the triclinic centrosymmetric space group $P\bar{1}$ with one independent donor in the asymmetric unit and the anion located on an inversion centre.[20] An interesting feature of these salts concerns the templating role of the PF_6^- anion through the establishment of C–H···F hydrogen bonding, leading to packings where donor layers are interconnected *via* the anions, all the fluorine atoms being involved in hydrogen bonding with either vinyl C=CH, methyne CH_{Me} or methyl protons. The final architectures very likely result from a delicate balance between these anion–donor hydrogen bonding and van der Waals S···S and orbital overlap interactions typical for oxidized TTF donors. We hypothesize that the massive difference in packing, and subsequently in transport properties, between the racemic and enantiopure salts finds its origin in this competition of intermolecular interactions. Thus, the use of the bigger congeners AsF_6^- and SbF_6^- could possibly influence on the stability of one or the

[a] *Université d'Angers, CNRS, Laboratoire MOLTECH-Anjou, UMR 6200, UFR Sciences, Bât. K, 2 Bd. Lavoisier, 49045 Angers, France. E-mail: narcis.avarvari@univ-angers.fr*
[b] *Laboratoire de Physique des Solides, Université Paris-Sud, UMR 8502, Bât. 510, 91405 Orsay, France*
[c] *Institut de Ciència de Materials de Barcelona (CSIC), Campus de la UAB, E-08193 Bellaterra, Spain*

† Electronic supplementary information (ESI) available. CCDC 1498583–1498588. For ESI and crystallographic data in CIF or other electronic format see DOI: 10.1039/c6cc06706a

other phase, *i.e.* monoclinic or triclinic, or maybe lead to completely new packings. Although generally for a given TTF type donor isostructural radical cation salts are observed within the series PF_6, AsF_6, SbF_6,[14b,21] there are only few cases,[22,23] to the best of our knowledge, where structural differences occur, including the (EDT-TTF)$_2XF_6$ (X = P, As) salts, where the one with PF_6 crystallized in an orthorhombic phase, while for the AsF_6 salt a second triclinic phase was observed.[22] We describe herein complete series of chiral radical cation salts of DM-EDT-TTF **1** with AsF_6^- and SbF_6^- anions and compare their structural features and conducting properties with the previously reported PF_6 counterparts.

Enantiopure and racemic donor **1**, prepared as previously described,[20] have been electrocrystallized in chloroform in the presence of [(*n*-Bu)$_4$N]XF_6 (X = As, Sb), the experimental conditions being identical in all the experiments with those employed for the PF_6 series.[20] Unexpectedly, while for the SbF_6^- anion only one crystalline phase has been obtained either for the enantiopure or the racemic donor, in the electrocrystallization cells with the AsF_6^- anion three types of crystals have been collected for enantiopure **1** and only one type when racemic **1** was used. The racemic AsF_6 and SbF_6 crystalline compounds are formulated as [(*rac*)-**1**]$_2XF_6$ (X = As, Sb) and are isostructural with the previous described PF_6 metallic salt.[20] They crystallize in the triclinic centrosymmetric space group $P\bar{1}$ with one independent donor molecule and half of anion, located on an inversion centre, in the asymmetric unit (see ESI† for details on single crystal X-ray measurements and Table S1 for crystal parameters). The central C=C bond lengths (1.371(6) Å and 1.369(5) Å for As and Sb, respectively) together with the internal C–S bond lengths, with an average value of 1.738 Å for both compounds, are in agreement with a +0.5 oxidation state of the donor and are comparable with the values measured for the PF_6 salt (Table S2, ESI†). The paramount role of the anion in the solid state architecture is evidenced through the complex set of hydrogen bonding interactions established between the fluorine atoms and CH_{vinyl}, CH_3 and CH_{Me} hydrogen atoms[24] leading to a packing where the anions are surrounded by donors, all the F atoms being involved in such short C–H···F contacts (Fig. 1 for SbF_6, Fig. S1 and S2 for PF_6 and AsF_6, and Table S3, ESI† for C–H···F distances and angles).

When comparing the three racemic structures there is a clear increase of the average C–H···F distances by changing the anion from PF_6 to AsF_6, and then to SbF_6 (Table S3, ESI†), while the intrastack intermolecular S···S distances remain essentially the same, in the range of 3.63–3.69 Å (*vide infra*), thus ensuring an optimum overlap between open shell species. As the average X–F bond length varies from 1.57 Å for P to 1.69 Å for As, and then to 1.85 Å for Sb, clearly the average C–H···F distance has to vary in the opposite way in order to keep the same arrangement of the donors, providing a fine control of the solid state architecture at the nanoscale level. However, this type of packing allows the involvement of the six fluorine atoms in short C–H···F contacts for the three anions in spite of their difference in size.

The situation is more complex for the enantiopure donors, since, as mentioned above, three different crystalline phases were obtained with the AsF_6 anion, while only one phase was isolated with SbF_6 and PF_6. As the enantiomeric pairs (*S*,*S*) and (*R*,*R*) were isostructural according to crystal cell determination, only the former will be detailed for the new phases. The enantiopure radical cation salt with the SbF_6 anion formulated as [(*S*,*S*)-**1**]$_2SbF_6$ is, interestingly, isostructural with the racemic phase, excepting the space group which is the non-centrosymmetric *P*1 in this case. The asymmetric unit contains one anion and two independent donor molecules **A** and **B** alternating in the stack (Fig. 2). This is in sharp contrast with the previous results in the PF_6 system where the monoclinic $P2_1$ structure was formed by 4 independent donor molecules and 2 anions.[20] Interestingly, the link between the two situations is provided by the AsF_6^- anion for which both crystalline phases are formed, *i.e.* triclinic *P*1 [(*S*,*S*)-**1**]$_2AsF_6$ and monoclinic $P2_1$ [(*S*,*S*)-**1**]$_4$-$(AsF_6)_2$, together with a third one, monoclinic $P2_1$ [(*S*,*S*)-**1**]$_2(AsF_6)_2$. The second is thus isostructural with the poorly conducting [(*S*,*S*)-**1**]$_4(PF_6)_2$ phase[20] and will not be further detailed. As for the racemic counterparts, in the enantiopure triclinic phases [(*S*,*S*)-**1**]$_2$-XF_6 (X = As, Sb) the bond distances indicate donor molecules in mixed valence state (Table S4, ESI†). While the packings of [(*rac*)-**1**]$_2$-SbF_6 (Fig. 1), [(*S*,*S*)-**1**]$_2SbF_6$ (Fig. 2) and [(*S*,*S*)-**1**]$_2AsF_6$ (Fig. S3, ESI†) present the same general features, some very fine differences in the C–H···F contacts can be disclosed, as the disposition of the stereogenic centres is different. Accordingly, the differences concern especially the interactions involving CH_{Me} and CH_3 groups. In order to satisfy at maximum the hydrogen bonding demand of the fluorine atoms, the donors slightly shift within the stack in order to optimize the C–H···F contacts (Table S5, ESI†).

The C–H···F distances are clearly larger in average for the AsF_6 salt (3.50 and 3.46 Å for H_3C···F and MeHC···F distances, respectively) than for the SbF_6 one (3.45 and 3.40 Å for H_3C···F and MeHC·····F distances, respectively) (Table S5, ESI†). Consequently, the fluorine atoms will be less involved in stabilizing hydrogen bonding contacts when going from SbF_6 to AsF_6 in the triclinic

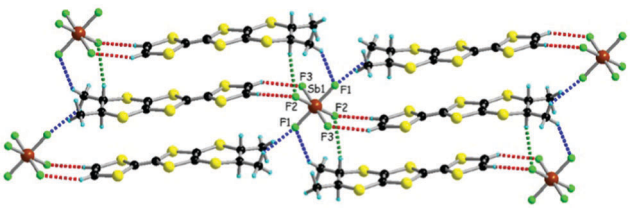

Fig. 1 Solid state structure of [(*rac*)-**1**]$_2SbF_6$, with an emphasis on the C–H···F short contacts (measured as C···F distances): red dotted lines for CH_{vinyl} (3.35 Å), blue dotted lines for CH_3 (3.31 and 3.49 Å) and green dotted line for CH_{Me} (3.35 Å). Only one conformation is shown for the dimethyl–ethylene bridge.

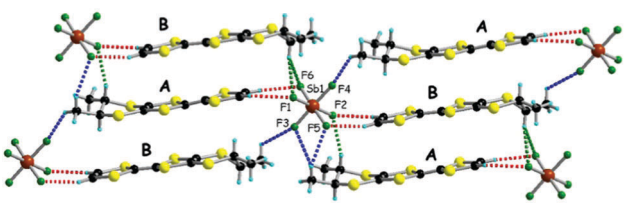

Fig. 2 Solid state structure of [(*S*,*S*)-**1**]$_2SbF_6$ with an emphasis on the C–H···F short contacts (measured as C···F distances): red dotted lines for CH_{vinyl} (3.23, 3.31, 3.42 and 3.45 Å), blue dotted lines for CH_3 (3.19, 3.44, 3.56 and 3.62 Å) and green dotted lines for CH_{Me} (3.23, 3.43 and 3.55 Å).

phase, therefore the donors will tend to adopt a different packing with the AsF_6 anion in the monoclinic 4 : 2 phase in order to maximize the hydrogen bonding interactions. This tendency is even higher for the PF_6^- anion, smallest of the series, exclusively providing the monoclinic phase in which all the fluorine atoms are involved in short C–H···F contacts (Fig. S4–S6, ESI†). Clearly, throughout this series, the chiral centres play the determining role in the fine tuning of the intermolecular interactions in the donors···anion aggregates, favouring either the triclinic (SbF_6), monoclinic (PF_6) or both (AsF_6) phases. Worth mentioning is that in the structures discussed thus far the methyl groups adopt equatorial (eq, eq) positions. However, in the third crystalline phase obtained with the AsF_6 anion the methyl groups show axial (ax, ax) disposition (Fig. S7 and S8, ESI†).[25] This compound, formulated as $[(S,S)\text{-}\mathbf{1}]_2(AsF_6)_2$ (its enantiomeric (*R*,*R*) counterpart is isostructural), crystallizes in the monoclinic non-centrosymmetric space group $P2_1$ with two independent donors and two anions in the asymmetric unit. The anions engage in hydrogen bonding interactions with the donors (Fig. S7, ESI†) which form strong dimers according to the very short intradimer S···S distances (Fig. S8, ESI†). The dimers further arrange in step-chains along the *a* direction. This type of arrangement is reminiscent with the one observed in the isostructural insulating radical cation salt $[(rac)\text{-}\mathbf{1}]ClO_4$.[2]

Single crystal temperature dependent resistivity measurements on triclinic $[\mathbf{1}]_2XF_6$ (X = As, Sb) show metallic behaviour in the high temperature range both for racemic (Fig. S9, ESI†) and enantiopure salts (Fig. 3).

Room temperature conductivity values are of the same order of magnitude for the enantiopure salts, *i.e.* 90 S cm^{-1} for SbF_6 and 70 S cm^{-1} for AsF_6, being slightly lower than those for the racemic salts, amounting to 250 S cm^{-1} for PF_6 and 125 S cm^{-1} for AsF_6. Most importantly, the enantiopure phases are metallic with a broad minimum of resistivity around 200 K then a metal to insulator (MI) transition takes place around 130–135 K. This temperature dependence of the resistivity is similar to that of racemic salts with only slightly higher transition temperatures (Fig. S9, ESI†).

The donor layers of triclinic $(DM\text{-}EDT\text{-}TTF)_2XF_6$ (X = P, As, Sb) are very similar. Those of the (*S*,*S*) salts contain two symmetry non-equivalent donors and six different donor···donor interactions labelled I to VI (Fig. 4). The donor layers of the racemic salts are very similar although with only one symmetry non-equivalent donor and five different interactions (*i.e.* interactions V and VI are equivalent for these salts). All of these layers are made of a series of parallel donor chains along the (*a*–*b*) direction. The strength of the different intermolecular interactions in all these salts can be assessed from the calculated $|\beta_{HOMO\text{–}HOMO}|$ interaction energies.[26]

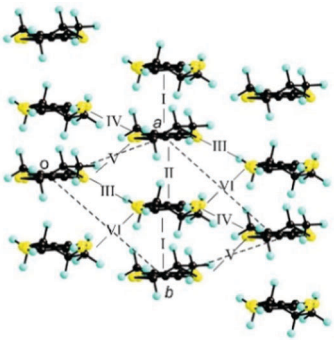

Fig. 4 Donor layer of (*S*,*S*)- and (*rac*)-$(DM\text{-}EDT\text{-}TTF)_2XF_6$ triclinic salts discussed in this work where the different intermolecular interactions are labelled.

The intrastack interactions (I and II) are considerably stronger than all the interstack ones and, although geometrically very different, their calculated $|\beta_{HOMO\text{–}HOMO}|$ values differ only by around 15% (Table S6 (ESI†) for $[(S,S)\text{-}\mathbf{1}]_2SbF_6$ and Tables S7–S10 (ESI†) for the other salts). Thus, from the viewpoint of the HOMO···HOMO interactions, these stacks are quite uniform chains of interacting HOMOs. Since the stacks run along the (*a*–*b*)-direction of the crystal structure, the two bands of the system (there are two donors per repeat unit of the donor layer) should exhibit strong dispersion along this direction (not far from $\Gamma \rightarrow S$ in reciprocal space) and considerably smaller along the perpendicular direction (not far from $\Gamma \rightarrow M$ in reciprocal space).

This is in fact what the calculated band structure (Fig. 5a for $[(S,S)\text{-}\mathbf{1}]_2SbF_6$, see ESI† for the other salts) shows. The inter-stack interactions (III to V/VI) are one order of magnitude smaller but their contributions add to give a quite sizeable dispersion to the upper band along the interstack direction (*i.e.* approximately along $\Gamma \rightarrow M$) so that the system should be seen as a series of substantially coupled and quite uniform stacks along the (*a*–*b*) direction. Because of the stoichiometry, the two HOMO bands (Fig. 5a) should contain one hole so that the upper band is half-filled. Since this band is quite dispersive, these salts are predicted to be metallic, in agreement with our conductivity measurements.

This analysis is confirmed by the calculated Fermi surface (Fig. 5b) which is built from a series of warped open lines perpendicular to the stacks direction. Thus, the present salts should be pseudo-one-dimensional metals at room temperature.

Can this analysis provide any guideline in trying to correlate the structural and transport properties of this family of salts? This is admittedly not an easy task because of the similarity in electronic structures and conductivity measurements (considering a larger number of crystals for every compound may be also important) along the series. Looking at the different interaction energies for all compounds of this series (Tables S6–S10, ESI†) we note that the two types of interstack interactions (III/IV and V/VI) are not only one order of magnitude smaller than the intrastack ones but their

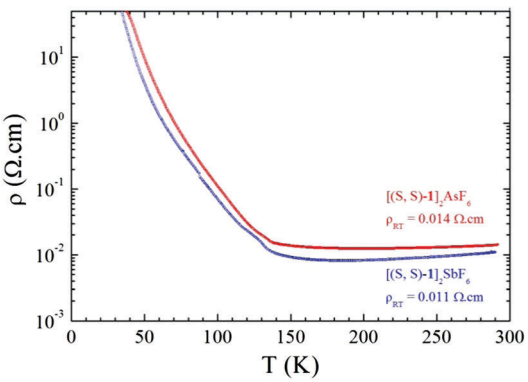

Fig. 3 Temperature dependence of the electrical resistivity ρ for a single crystal of $[(S,S)\text{-}\mathbf{1}]_2AsF_6$ (red line) and a single crystal of $[(S,S)\text{-}\mathbf{1}]_2SbF_6$ (blue line).

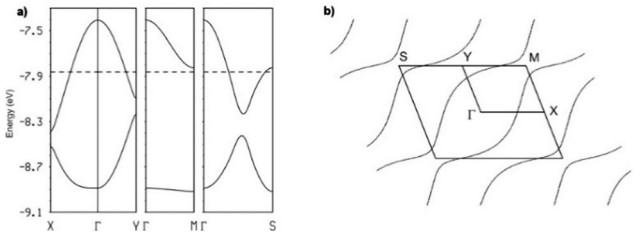

Fig. 5 Calculated band structure (a) and Fermi surface (b) for the donor layers of [(*S*,*S*)-**1**]$_2$SbF$_6$ at room temperature. The dashed line in (a) refers to the Fermi level and Γ = (0, 0), X = (a^*/2, 0), Y = (0, b^*/2), M = (a^*/2, b^*/2) and S = (−a^*/2, b^*/2).

variation along the series is also considerably smaller. Thus, the intrastack HOMO···HOMO interactions are those dominating the shape of the upper partially filled band, *i.e.* the transport properties of the salts. For chains like those along (*a*–*b*) in Fig. 4, with two different but strong interactions along the chain, the slope of the upper band around the Fermi level should be dominated by the strength of the weaker of the two interactions. Thus the $|\beta_{\text{HOMO-HOMO}}|$ value for interaction II should be an adequate electronic structure parameter allowing classifying the different salts according to their conductivity: larger values of this parameter should be associated with higher conductivities. Using this simple guideline and the calculated $|\beta_{\text{HOMO-HOMO}}|$ values it follows that: (i) the conductivity should decrease along a given type of salt when the size of the anion increases, (ii) for the same anion the (*rac*)-salts should be more conductive when there is no disorder. When examining the structural origin of the variation in the $|\beta_{\text{HOMO-HOMO}}|$ values it is clear that the main factor lies in the evolution of the intermolecular S···S contacts and to a lesser extent the slight sliding motions induced by the different anions. Thus, the chiral information is transmitted to the conductivity carriers through the $F_{(\text{anion})}\cdots H_{(\text{donor})}$ interactions which, in turn, together with the anion size, influence the intrastack interactions, and, more specially, the weaker of the two intrastack interactions. This simple approach represents a step further with respect to simple anion size based ideas since suggests differences between the enantiopure and racemic salts. The presently known conductivity results are grossly in agreement with these ideas although more extensive work is in order. In particular the values for the SbF_6 salts may require further attention.

Further work in this series will be devoted to the investigation of the conducting properties of the enantiopure salts under magnetic field and the use of variable composition alloys of XF_6 anions in order to have a complete picture of these intriguing systems.

This work was supported in France by the ANR (Project 09-BLAN-0045-01), the CNRS and the University of Angers. Work in Spain was supported by the Spanish MINECO through Grant FIS2015-64886-C5-4-P and the Severo Ochoa Centers of Excellence Program under Grant SEV-2015-0496. We warmly thank M. Allain (MOLTECH-Anjou, Angers) for valuable technical help with the X-ray analysis.

Notes and references

1 N. Avarvari and J. D. Wallis, *J. Mater. Chem.*, 2009, **19**, 4061–4076.
2 F. Pop, P. Auban-Senzier, E. Canadell, G. L. J. A. Rikken and N. Avarvari, *Nat. Commun.*, 2014, **5**, 3757.
3 J.-P. Griffiths, H. Nie, R. J. Brown, P. Day and J. D. Wallis, *Org. Biomol. Chem.*, 2005, **3**, 2155–2166.
4 S. Yang, A. C. Brooks, L. Martin, P. Day, H. Li, P. Horton, L. Male and J. D. Wallis, *CrystEngComm*, 2009, **11**, 993–996.
5 F. Riobé and N. Avarvari, *Chem. Commun.*, 2009, 3753–3755.
6 I. Awheda, S. J. Krivickas, S. Yang, L. Martin, M. A. Guziak, A. C. Brooks, F. Pelletier, M. Le Kerneau, P. Day, P. N. Horton, H. Akutsu and J. D. Wallis, *Tetrahedron*, 2013, **69**, 8738–8750.
7 M. Chas, M. Lemarié, M. Gulea and N. Avarvari, *Chem. Commun.*, 2008, 220–222.
8 M. Hasegawa, Y. Sone, S. Iwata, H. Matsuzawa and Y. Mazaki, *Org. Lett.*, 2011, **13**, 4688–4691.
9 (*a*) R. Gómez, J. L. Segura and N. Martin, *J. Org. Chem.*, 2000, **65**, 7566–7574; (*b*) A. Saad, F. Barrière, E. Levillain, N. Vanthuyne, O. Jeannin and M. Fourmigué, *Chem. – Eur. J.*, 2010, **16**, 8020–8028.
10 T. Biet, A. Fihey, T. Cauchy, N. Vanthuyne, C. Roussel, J. Crassous and N. Avarvari, *Chem. – Eur. J.*, 2013, **19**, 13160–13167.
11 K. Kobayakawa, M. Hasegawa, H. Sasaki, J. Endo, H. Matsuzawa, K. Sako, J. Yoshida and Y. Mazaki, *Chem. – Asian J.*, 2014, **9**, 2751–2754.
12 F. Pop, C. Melan, I. Danila, M. Linares, D. Beljonne, D. B. Amabilino and N. Avarvari, *Chem. – Eur. J.*, 2014, **20**, 17443–17453.
13 (*a*) S. Matsumiya, A. Izuoka, T. Sugawara, T. Taruishi, Y. Kawada and M. Tokumoto, *Bull. Chem. Soc. Jpn.*, 1993, **66**, 1949–1954; (*b*) F. Pop, M. Allain, P. Auban-Senzier, J. Martínez-Lillo, F. Lloret, M. Julve, E. Canadell and N. Avarvari, *Eur. J. Inorg. Chem.*, 2014, 3855–3862.
14 (*a*) J. R. Galán-Mascarós, E. Coronado, P. A. Goddard, J. Singleton, A. I. Coldea, J. D. Wallis, S. J. Coles and A. Alberola, *J. Am. Chem. Soc.*, 2010, **132**, 9271–9273; (*b*) S. Yang, F. Pop, C. Melan, A. C. Brooks, L. Martin, P. Horton, P. Auban-Senzier, G. L. J. A. Rikken, N. Avarvari and J. D. Wallis, *CrystEngComm*, 2014, **16**, 3906–3916; (*c*) M. Atzori, F. Pop, P. Auban-Senzier, R. Clérac, E. Canadell, M. L. Mercuri and N. Avarvari, *Inorg. Chem.*, 2015, **54**, 3643–3653.
15 J. D. Dunitz, A. Karrer and J. D. Wallis, *Helv. Chim. Acta*, 1986, **69**, 69–70.
16 (*a*) G. L. J. A. Rikken, J. Fölling and P. Wyder, *Phys. Rev. Lett.*, 2001, **87**, 236602; (*b*) V. Krstic, S. Roth, M. Burghard, K. Kern and G. L. J. A. Rikken, *J. Chem. Phys.*, 2002, **117**, 11315–11319.
17 C. Réthoré, N. Avarvari, E. Canadell, P. Auban-Senzier and M. Fourmigué, *J. Am. Chem. Soc.*, 2005, **127**, 5748–5749.
18 F. Pop, S. Laroussi, T. Cauchy, C. J. Gómez-García, J. D. Wallis and N. Avarvari, *Chirality*, 2013, **25**, 466–474.
19 A. M. Madalan, C. Réthoré, M. Fourmigué, E. Canadell, E. B. Lopes, M. Almeida, P. Auban-Senzier and N. Avarvari, *Chem. – Eur. J.*, 2010, **16**, 528–537.
20 F. Pop, P. Auban-Senzier, A. Frąckowiak, K. Ptaszyński, I. Olejniczak, J. D. Wallis, E. Canadell and N. Avarvari, *J. Am. Chem. Soc.*, 2013, **135**, 17176–17186.
21 (*a*) K. Bechgaard, C. S. Jacobsen, K. Mortensen, H. J. Pedersen and N. Thorup, *Solid State Commun.*, 1980, **33**, 1119–1125; (*b*) J. Tarrés, N. Santaló, M. Mas, E. Molins, J. Veciana, C. Rovira, S. Yang, H. Lee, D. O. Cowan, M.-L. Doublet and E. Canadell, *Chem. Mater.*, 1995, **7**, 1558–1567; (*c*) T. Shirahata, K. Shiratori, S. Kumeta, T. Kawamoto, T. Ishikawa, S. Koshihara, Y. Nakano, H. Yamochi, Y. Misaki and T. Mori, *J. Am. Chem. Soc.*, 2012, **134**, 13330–13340.
22 R. Kato, H. Kobayashi and A. Kobayashi, *Chem. Lett.*, 1989, 781–784.
23 T. Shirahata, M. Kibune and T. Imakubo, *J. Mater. Chem.*, 2005, **15**, 4399–4402.
24 (*a*) G. R. Desiraju and T. Steiner, *The Weak Hydrogen Bond in Structural Chemistry and Biology*, OUP, Chichester, 1999; (*b*) G. R. Desiraju, *Acc. Chem. Res.*, 2002, **35**, 565–573; (*c*) G. R. Desiraju, *Acc. Chem. Res.*, 1996, **29**, 441–449.
25 F. Pop, P. Batail and N. Avarvari, *Crystals*, 2016, **6**, 8.
26 M.-H. Whangbo, J. M. Williams, P. C. W. Leung, M. A. Beno, T. J. Emge and H. H. Wang, *Inorg. Chem.*, 1985, **24**, 3500–3502.